



**IAEA**

International Atomic Energy Agency

INDC(NDS)-0554  
Distr. G+NM

## **INDC International Nuclear Data Committee**

### **Nuclear Level Densities of $^{116}\text{Sb}$ , $^{118}\text{Sb}$ , $^{122}\text{Sb}$ , $^{124}\text{Sb}$ , $^{165}\text{Er}$ and $^{181}\text{W}$ Derived from Neutron Evaporation Spectra in the (p,n) Reaction**

B.V. Zhuravlev

State Scientific Centre of the Russian Federation  
Institute of Physics and Power Engineering  
249033 Obninsk, Kaluga Region, Russian Federation

April 2009

Selected INDC documents may be downloaded in electronic form from [http://www-nds.iaea.org/indc\\_sel.html](http://www-nds.iaea.org/indc_sel.html) or sent as an e-mail attachment. Requests for hardcopy or e-mail transmittal should be directed to [services@iaeand.iaea.org](mailto:services@iaeand.iaea.org) or to:

Nuclear Data Section  
International Atomic Energy Agency  
PO Box 100  
Wagramer Strasse 5  
A-1400 Vienna  
Austria

Produced by the IAEA in Austria  
April 2009

# Nuclear Level Densities of $^{116}\text{Sb}$ , $^{118}\text{Sb}$ , $^{122}\text{Sb}$ , $^{124}\text{Sb}$ , $^{165}\text{Er}$ and $^{181}\text{W}$ Derived from Neutron Evaporation Spectra in the (p,n) Reaction

B.V. Zhuravlev  
State Scientific Centre of the Russian Federation  
Institute of Physics and Power Engineering  
249033 Obninsk, Kaluga Region, Russian Federation

## Abstract

Nuclear level density data for  $^{116}\text{Sb}$ ,  $^{118}\text{Sb}$ ,  $^{122}\text{Sb}$ ,  $^{124}\text{Sb}$ ,  $^{165}\text{Er}$  and  $^{181}\text{W}$  nuclei have been compiled from neutron evaporation spectra in the (p,n) reaction. Excitation functions, neutron spectra and angular distributions in the (p,n) reaction were measured on  $^{116}\text{Sn}$ ,  $^{118}\text{Sn}$ ,  $^{122}\text{Sn}$ ,  $^{124}\text{Sn}$ ,  $^{165}\text{Ho}$  and  $^{181}\text{Ta}$  nuclei in the proton energy range of 7 to 11 MeV. The measurements were performed by time-of-flight fast neutron spectrometry on the EGP-15 pulsed tandem accelerator of IPPE. Analysis of the measured data was carried out on the basis of the statistical equilibrium and pre-equilibrium models of nuclear reactions. The calculations involved the adoption of the exact formalism of the statistical theory as given by Hauser-Feshbach. Nuclear level densities of  $^{116}\text{Sb}$ ,  $^{118}\text{Sb}$ ,  $^{122}\text{Sb}$ ,  $^{124}\text{Sb}$ ,  $^{165}\text{Er}$  and  $^{181}\text{W}$  and their energy dependencies were determined.

April 2009



## TABLE OF CONTENTS

1. INTRODUCTION .....	7
2. EXPERIMENTS.....	7
3. DATA ANALYSIS .....	8
4. RESULTS.....	12
5. CONCLUSIONS.....	12



# NUCLEAR LEVEL DENSITIES OF $^{116}\text{Sb}$ , $^{118}\text{Sb}$ , $^{122}\text{Sb}$ , $^{124}\text{Sb}$ , $^{165}\text{Er}$ AND $^{181}\text{W}$ DERIVED FROM NEUTRON EVAPORATION SPECTRA IN THE (p,n) REACTION

*B.V. Zhuravlev*

## Introduction

Nuclear level densities are of considerable interest in nuclear physics because these data have assisted greatly in the creation of a consistent theoretical description of excited nucleus properties and aided significantly in nuclear reaction cross-section calculations in terms of the statistical model for many branches of nuclear physics, nuclear astrophysics and applied areas. The general features of nuclear level density are known, but there are considerable uncertainties in the functional forms, in particular, connected with shell effects, the coherent effects of collective nature, residual interaction, (N-Z) dependence, etc. Required accuracies of level densities for nuclear cross-section calculations are  $\sim 10\%$  over a wide range of excitation energy from 0.1 to 20 MeV, and the existing data often differ by a factor of 1.5. Experimental nuclear level densities for many nuclei are derived from the analysis of neutron resonance data and low-lying states. But this information is limited to rather narrow ranges of excitation energy and spin, and extrapolation can lead to significant errors in both the absolute value of nuclear level density and energy dependence, especially in the transition field from well-identified discrete states to the continuum part of the excitation spectrum. Obviously, other experimental methods of nuclear level density determination need to be developed with much wider ranges of excitation energy and spin. One source of information on nuclear level density between the resolved states and neutron binding energy at an accuracy comparable with neutron resonance data are the spectra of particles emitted in nuclear reactions. The type of reaction and energy of incident particles should be chosen so that the contribution of nonequilibrium processes is at a minimum. For medium and heavy nuclei, these conditions are best satisfied by the (p,n) reaction at proton energies up to 11 MeV. Data on the nuclear level density of  $^{116}\text{Sb}$ ,  $^{118}\text{Sb}$ ,  $^{122}\text{Sb}$ ,  $^{124}\text{Sb}$ ,  $^{165}\text{Er}$  and  $^{181}\text{W}$  from neutron evaporation spectra in the (p,n) reaction [1-3] have been compiled, and descriptions of the measurements and data analysis are presented.

## Experiments

Neutron spectra from the (p,n) reaction on nuclei of  $^{116}\text{Sn}$ ,  $^{118}\text{Sn}$ ,  $^{122}\text{Sn}$ ,  $^{124}\text{Sn}$ ,  $^{165}\text{Ho}$  and  $^{181}\text{Ta}$  have been measured at proton energies between 7 and 11 MeV. The measurements of neutron spectra were performed by means of a time-of-flight fast neutron spectrometer on the EGP-15 pulsed tandem accelerator of IPPE at an angle range of 20 to  $140^\circ$ . Targets consisted of self-supporting metal foils with thicknesses of 4.00, 4.98, 2.10, 3.80, 13.66 and 18.00 mg/cm<sup>2</sup> and enrichments of 97.8, 98.7, 97.5, 98.3, 99.9 and 99.9 % for  $^{116}\text{Sn}$ ,  $^{118}\text{Sn}$ ,  $^{122}\text{Sn}$ ,  $^{124}\text{Sn}$ ,  $^{165}\text{Ho}$  and  $^{181}\text{Ta}$ , respectively. Neutrons were detected by means of a scintillation detector consisting of a stilben crystal (d-40mm, h-40mm) and FEU-143 photomultiplier. Background was decreased by a combination of massive shielding and electronic discrimination of the gamma rays. The detector efficiency was determined from measurements of the  $^{252}\text{Cf}$  prompt fission neutron spectrum by means of the time-of-flight method, with a specially-designed fast ionization chamber in the same geometry as the main experiment. Detector efficiency was reduced from a comparison of the measured spectrum with a standard spectrum [4]. Spectrometer stability and the quality of the beam pulses were controlled by additional detectors based on a fast plastic scintillator and FEU-82 photomultiplier, which aided in the detection of  $\gamma$  quanta from

the Faraday-cup beam-stopper. The electronic circuits of the spectrometer, detection, storage and data processing circuits are presented in Fig. 1 and are described in detail in Ref. [5]. Neutron spectrum measurements were undertaken with and without the target in place, at the same proton flux. The background was small and virtually uncorrelated over time. A combination of high resolution ( $\sim 0.6$  ns/m) and stability of the time-of-flight spectrometer permitted the reliable identification of discrete low-lying levels together with the continuum neutron spectra. Typical angle-integrated neutron emission spectra for the  $^{118}\text{Sn}(p,n)$  reaction at several incident-proton energies are presented in Fig. 2.

### Data analysis

Nuclear level density determination from emission spectra is based on the fact that nuclear level density is one of the most critical components of statistical model calculations and the analysis of compound nucleus reactions by means of the Hauser-Feshbach model. The cross section for the population of the residual nucleus level by the emission of neutrons from the compound nucleus is given by the equation:

$$\sigma(E_p, E_n) = \sum_{J,\pi} \sigma_{\text{CN}}(E_p) \cdot [\Gamma_n(U, J, \pi, U_r, I_r, \pi_r) / \Gamma(U, J, \pi)],$$

where  $U, J, \pi$  are the excitation energy, angular momentum and parity of the compound nucleus,

$U_r, I_r, \pi_r$  are the excitation energy, angular momentum and parity of the residual nucleus,

$E_p, E_n$  are the energies of protons and neutrons,

$\sigma_{\text{CN}}(E_p)$  is the compound nucleus formation cross section with spin  $J$  and parity  $\pi$ ,

$\Gamma_n(U, J, \pi, U_r, I_r, \pi_r)$  is the decay width of the compound nucleus to the level of the residual nucleus by emission of neutrons, and

$\Gamma(U, J, \pi)$  is the total decay width of the compound nucleus.

Differential neutron emission cross section for population of continuum states is defined as:

$$d\sigma(E_p, E_n) / dE_n = \sum_{J,\pi} \sigma_{\text{CN}}(E_p) \cdot [\sum_{I_r,\pi_r} \Gamma_n(U, J, \pi, U_r, I_r, \pi_r) \cdot \rho(U_r, I_r, \pi_r) / \Gamma(U, J, \pi)],$$

where  $\rho(U_r, I_r, \pi_r)$  is the level density of the residual nucleus reached by the emission of the neutrons.





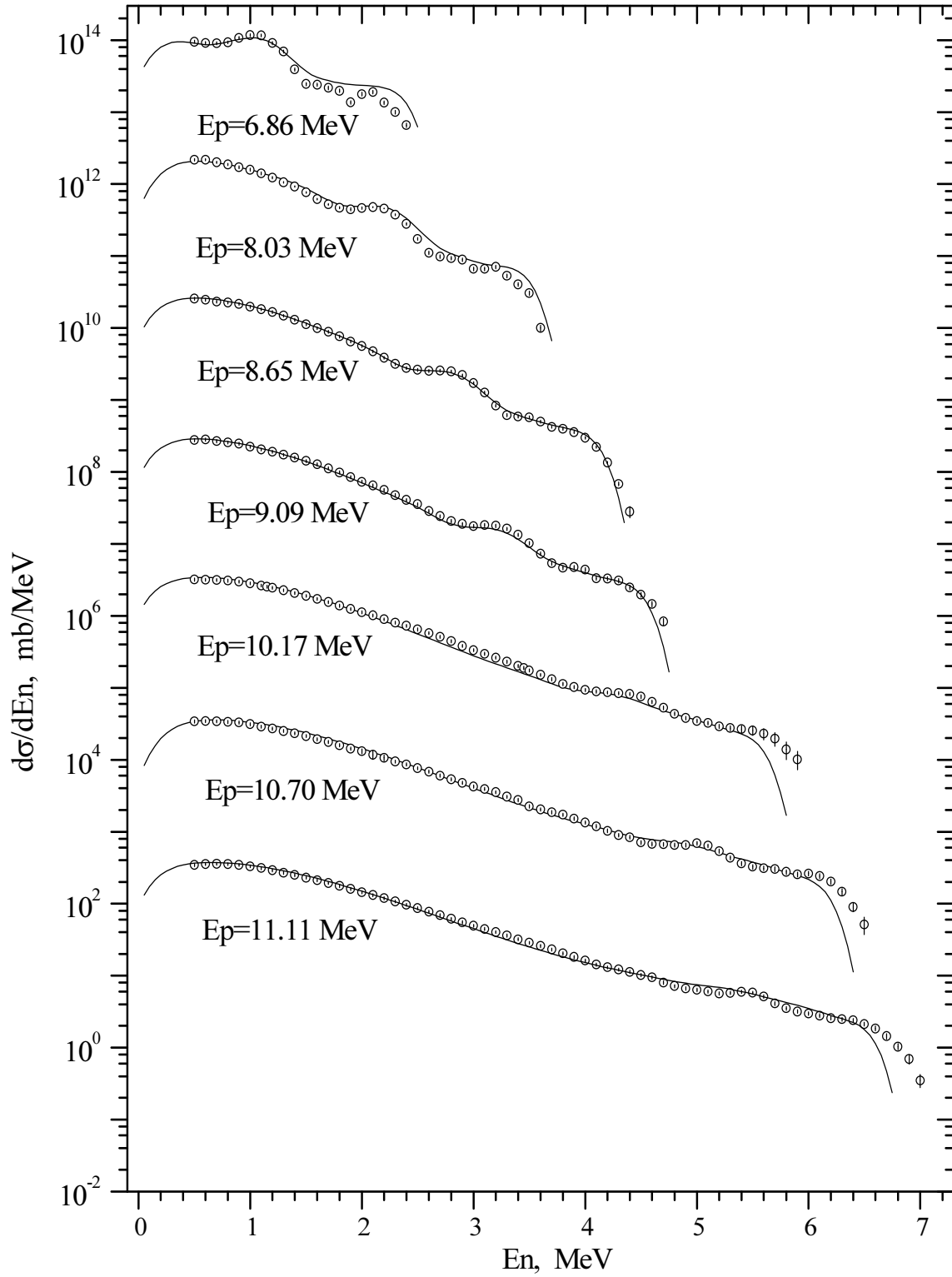


**FIG. 2.** Angle-integrated neutron emission spectra from the  $^{118}\text{Sn}(p,n)^{118}\text{Sb}$  reaction – symbols are experimental data, curves are fitted results. Plots are shifted by 100 units each starting from the bottom for better visibility.

Determinations of nuclear level density consists of the following:

1. The model parameters of the level density are adjusted such that the cross section calculated by means of Hauser-Feshbach formula fits the measured value in the energy range of well-known low-lying levels. Thus, the total decay width of the compound nucleus is determined.
2. The chosen model of the level density is adopted at first, and the absolute values of the level density in subsequent iterations to calculate the differential cross section for the continuum, while the absolute level density is determined over a wide range of excitation energies from the best fit with the measured spectra.

A good description is required in a high-energy part of the neutron spectra in order to determine the nuclear level density. Normalization of the calculated cross sections with respect to the experimental data in the range of well-known low-lying levels permits the determination of the Hauser-Feshbach denominator, i.e. the total width of the compound nucleus. Thus, the absolute level density can be derived from a comparison of the calculated and measured spectra in the experimental range of the excitation energies:

$$\rho(U) = \rho(U)_{\text{assumed}} \cdot (d\sigma/dE_n)_{\text{measured}} / (d\sigma/dE_n)_{\text{calculated}}$$

This equation is based on the assumption that differences between the calculated and measured cross sections in the continuum arise mainly from differences in the nuclear level density. Other quantities are assumed to impact in terms of the uncertainties in the nuclear level density.

The whole range of the excitation energy was divided into a number of equally-spaced quasi-discrete levels ( $\sim 0.2$  MeV per energy bin) for the calculation of the differential neutron emission cross sections in the continuum. Within each interval there are assumed to be up to 30 different spin states of one parity and the same number of the other parity with a probability of  $\rho(U, J)$ . Such quasi-discrete levels were processed by the code as normal discrete states with effective transmission coefficients. All statistical model calculations have been carried out with the GNASH and PEAK-98 codes [6, 7]. A search of the nuclear level density is initially carried out from analyses of measured neutron spectra in the (p,n) reaction at low-incident proton energies. The emission cross section of the (p,n) reaction is dominated by the statistical equilibrium mechanism. At greater proton energies, the contributions of the pre-equilibrium mechanism and the secondary emission of neutrons through (p,pn) and (p,2n) reactions were taken into account. Once the maximum excitation energy is reached, the next iteration begins. The  $\chi^2$  criterion was used to assess the agreement between the experimental and fitted spectra. At low excitation energies, the transitions to well-identified discrete levels of the residual nucleus were calculated. The resulting cross sections have been averaged over the excitation energy based on a normal (Gaussian) distribution in which the dispersion (width) of the distribution corresponds to the resolution of the spectrometer. Independently-determined neutron and proton optical potentials valid in the relevant energy range are used to determine a reliable nuclear level density from observed neutron spectra. A search of the nucleon optical parameters was carried out by assessing all accessible experimental data on neutron and proton scattering and total cross sections. The input level density parameters in all compound nucleus decay channels used in the calculations were chosen to guarantee that the calculated nuclear level density agreed with the low-lying levels and neutron resonance data [8, 9]. Contributions of non-equilibrium reaction mechanism were calculated by means of the exciton pre-equilibrium model as formulated by Kalbach in the PRECO-B code [10].

## Results

Typical best-fit emission spectra for the  $^{118}\text{Sn}(p,n)^{118}\text{Sb}$  reaction obtained at several incident proton energies are shown in Fig. 2. Comparison of the calculated and measured neutron spectra demonstrates good fits for both the discrete-level and continuum segments. The extracted level densities for residual  $^{116}\text{Sb}$ ,  $^{118}\text{Sb}$ ,  $^{122}\text{Sb}$ ,  $^{124}\text{Sb}$ ,  $^{165}\text{Er}$  and  $^{181}\text{W}$  nuclei excited in the reactions under study are presented in Figs. 3-8 and Tables 1-6. Structure observed for Sb nuclei at excitation energies below 2 MeV is associated with the shell inhomogeneity of the single-particle spectrum for nuclei near magic number  $Z = 50$  and are in agreement with low-lying level data. The total uncertainties of the level densities were evaluated from the uncertainties of the neutron spectral measurements of  $\sim 4\%$  to  $15\%$ , uncertainties of neutron optical potential of  $\sim 7\%$  to  $10\%$ , uncertainties of spin dependence of  $\sim 7\%$ , and uncertainties due to preequilibrium effects of  $\sim 5\%$  to  $7\%$ . As a result, the total uncertainties of the nuclear level density determination were evaluated to be  $\sim 15\%$  for  $^{116}\text{Sb}$ ,  $^{118}\text{Sb}$ ,  $^{122}\text{Sb}$  and  $^{124}\text{Sb}$ ,  $\sim 20\%$  for  $^{165}\text{Er}$ , and  $\sim 17\%$  for  $^{181}\text{W}$ .

## Conclusions

The nuclear level density data for  $^{116}\text{Sb}$ ,  $^{118}\text{Sb}$ ,  $^{122}\text{Sb}$ ,  $^{124}\text{Sb}$ ,  $^{165}\text{Er}$  and  $^{181}\text{W}$  from neutron evaporation spectra in the (p,n) reaction [1-3] have been compiled, and the description of the measurements and data analysis are presented. Differential neutron emission spectra in the (p,n) reaction on  $^{116}\text{Sn}$ ,  $^{118}\text{Sn}$ ,  $^{122}\text{Sn}$ ,  $^{124}\text{Sn}$ ,  $^{165}\text{Ho}$  and  $^{181}\text{Ta}$  have been measured and analyzed in terms of the statistical equilibrium and pre-equilibrium models of nuclear reactions. The absolute nuclear level densities of  $^{116}\text{Sb}$ ,  $^{118}\text{Sb}$ ,  $^{122}\text{Sb}$ ,  $^{124}\text{Sb}$ ,  $^{165}\text{Er}$  and  $^{181}\text{W}$  and their energy dependence have been determined.

## References

1. B.V. Zhuravlev, A.A. Lychagin, N.N. Titarenko, *Yad. Fiz.* 2006, vol. 69, № 3, pp. 387-394.
2. B.V. Zhuravlev, *Izv. Akad. Nauk, Ser. Fiz.* 1999, vol. 63, № 1, pp. 148-152.
3. B.V. Zhuravlev, N.N. Titarenko, V.I. Trykova, *Yad. Fiz.* 1990, vol. 51, № 2, pp. 311-317.
4. W. Mannhart, IAEA-TECDOC-410, Vienna, 1987, p. 158.
5. V.G. Demenkov, B.V. Zhuravlev, A.A. Lychagin, V.I. Mil'shin, V.I. Trykova, *Instruments and Experimental Techniques*, vol.38, № 3, 1995, pp. 314-318.
6. P.G. Young, E.D. Arthur, M.B. Chadwick, *Proc. IAEA Workshop on Nuclear Reaction Data and Nuclear Reactors*, Trieste, Italy, 15 April – 17 May 1996, vol.1, p. 227. Eds. A. Gandini and G. Reffo, World Scientific, Singapore, 1998.
7. N.N. Titarenko, preprint IPPE-2289, Obninsk-1992; B.V. Zhuravlev, N.N. Titarenko, preprint IPPE-2819, Obninsk-2000.
8. ENSDF - evaluated nuclear structure and decay data.
9. G. Reffo, "Chapter: Level Densities", IAEA-TECDOC-1034, 1998.
10. C. Kalbach, Saclay Report DPh-N/BE/74/3, 1974.

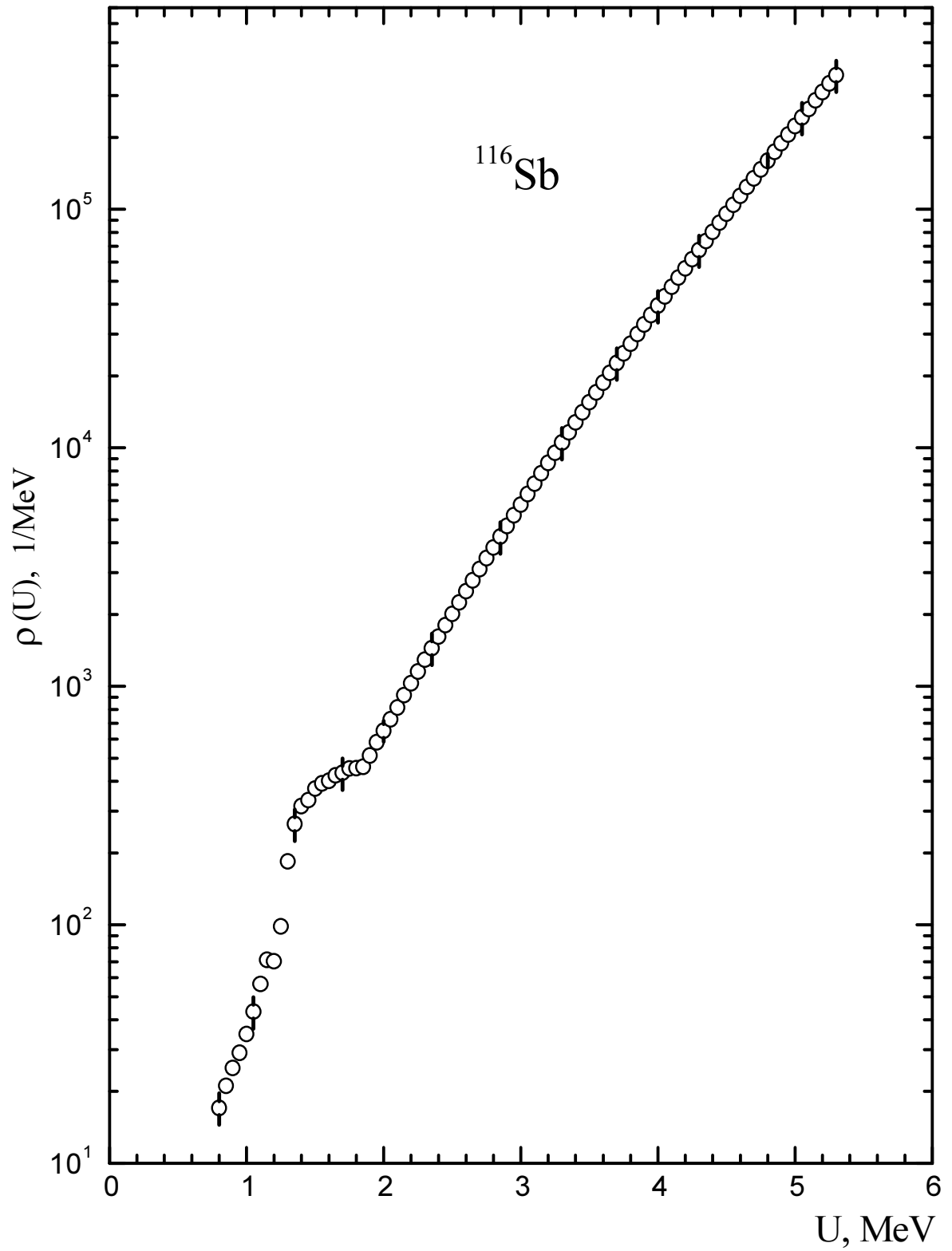


**FIG. 3.** Nuclear level density of  $^{116}\text{Sb}$

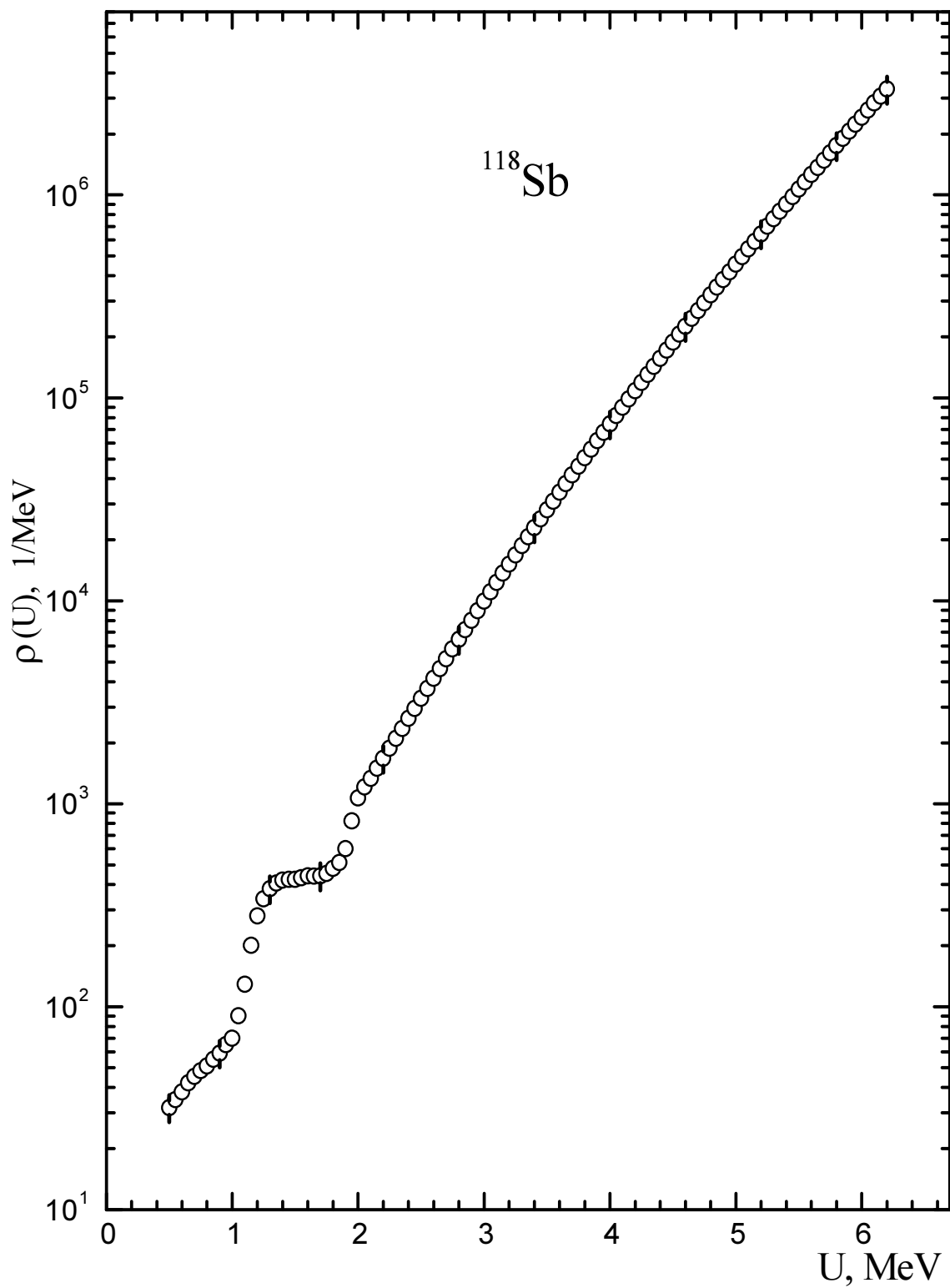


**FIG. 4.** Nuclear level density of  $^{118}\text{Sb}$

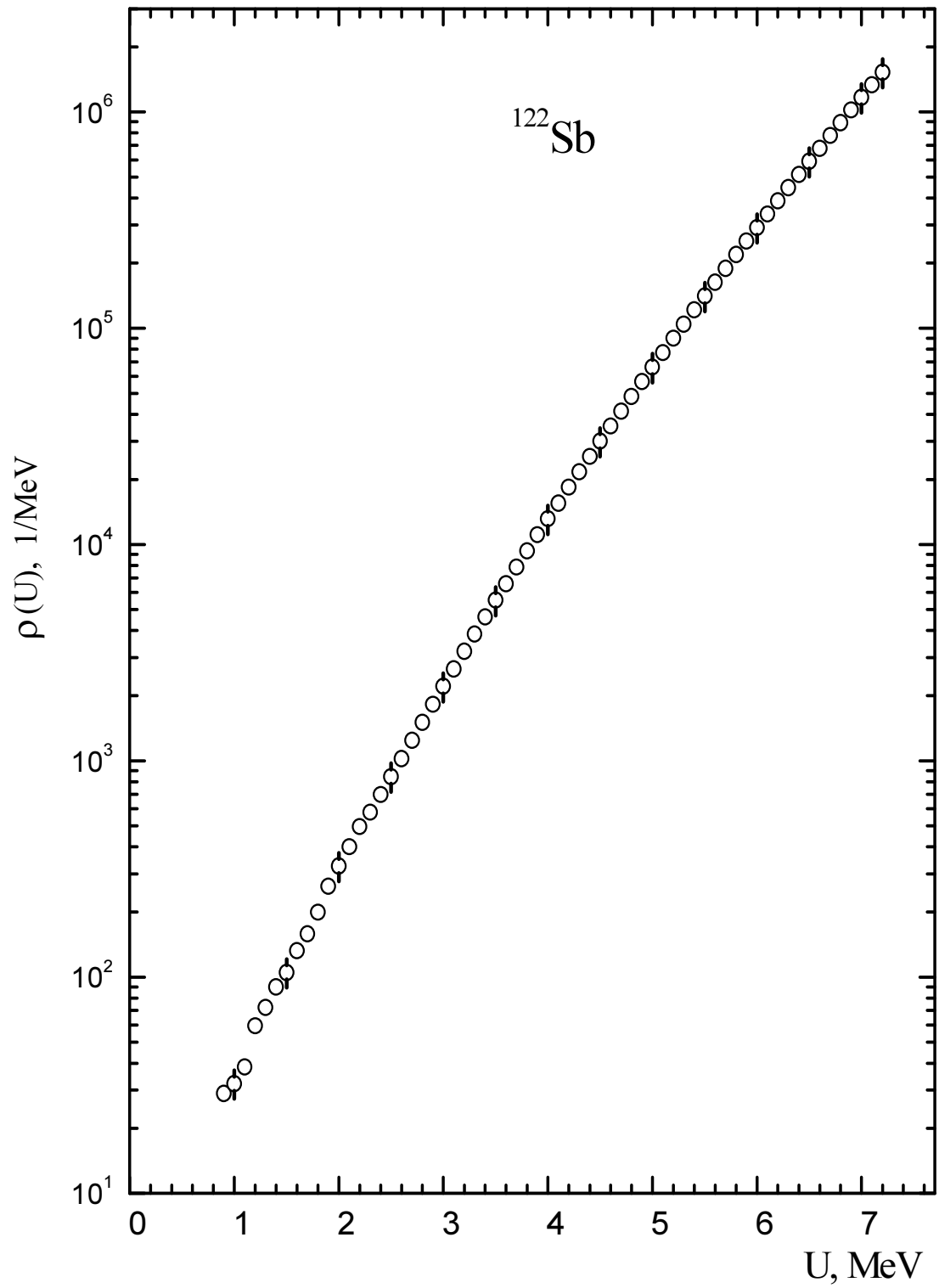


**FIG. 5.** Nuclear level density of  $^{122}\text{Sb}$

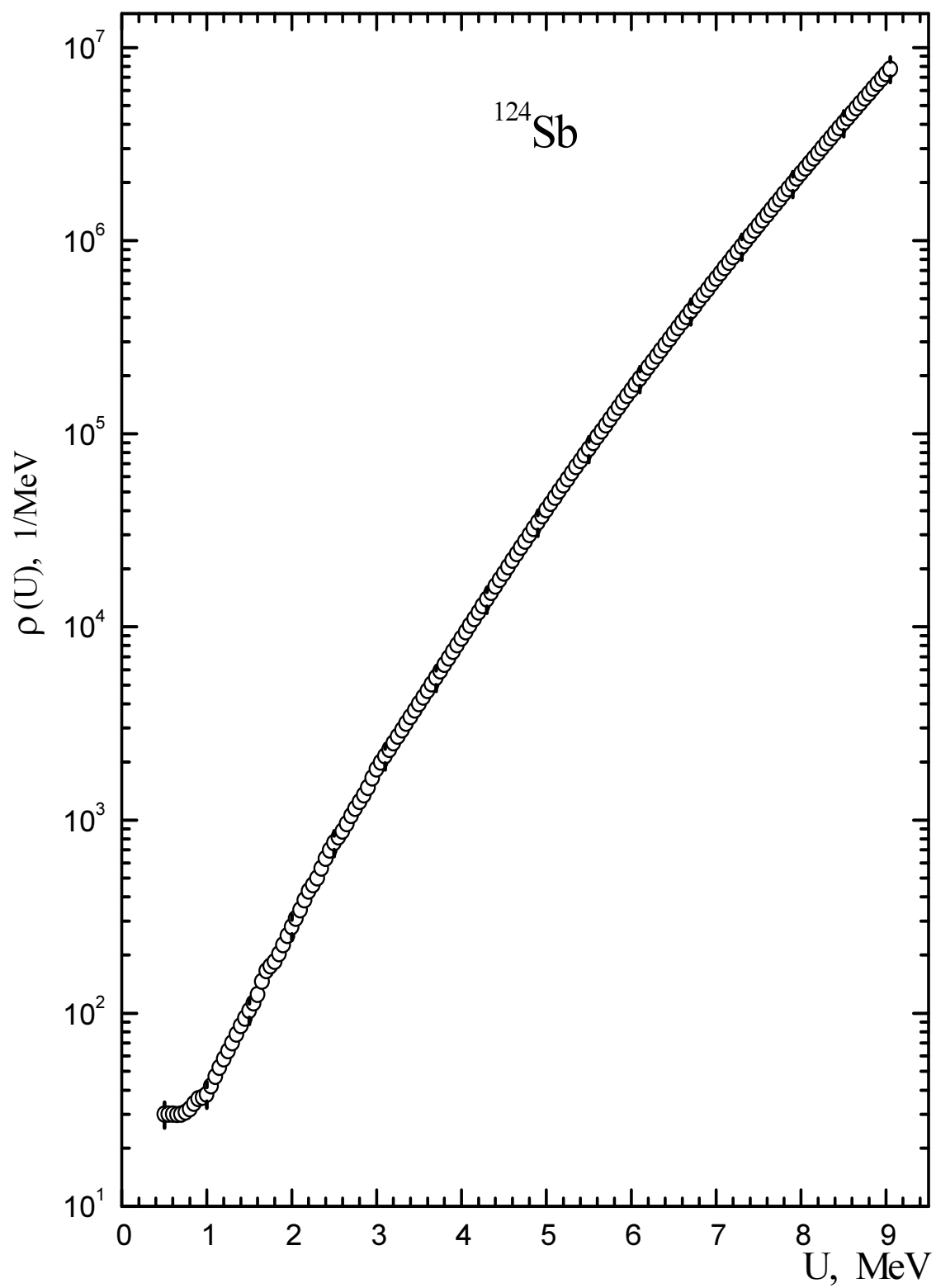


**FIG. 6.** Nuclear level density of  $^{124}\text{Sb}$



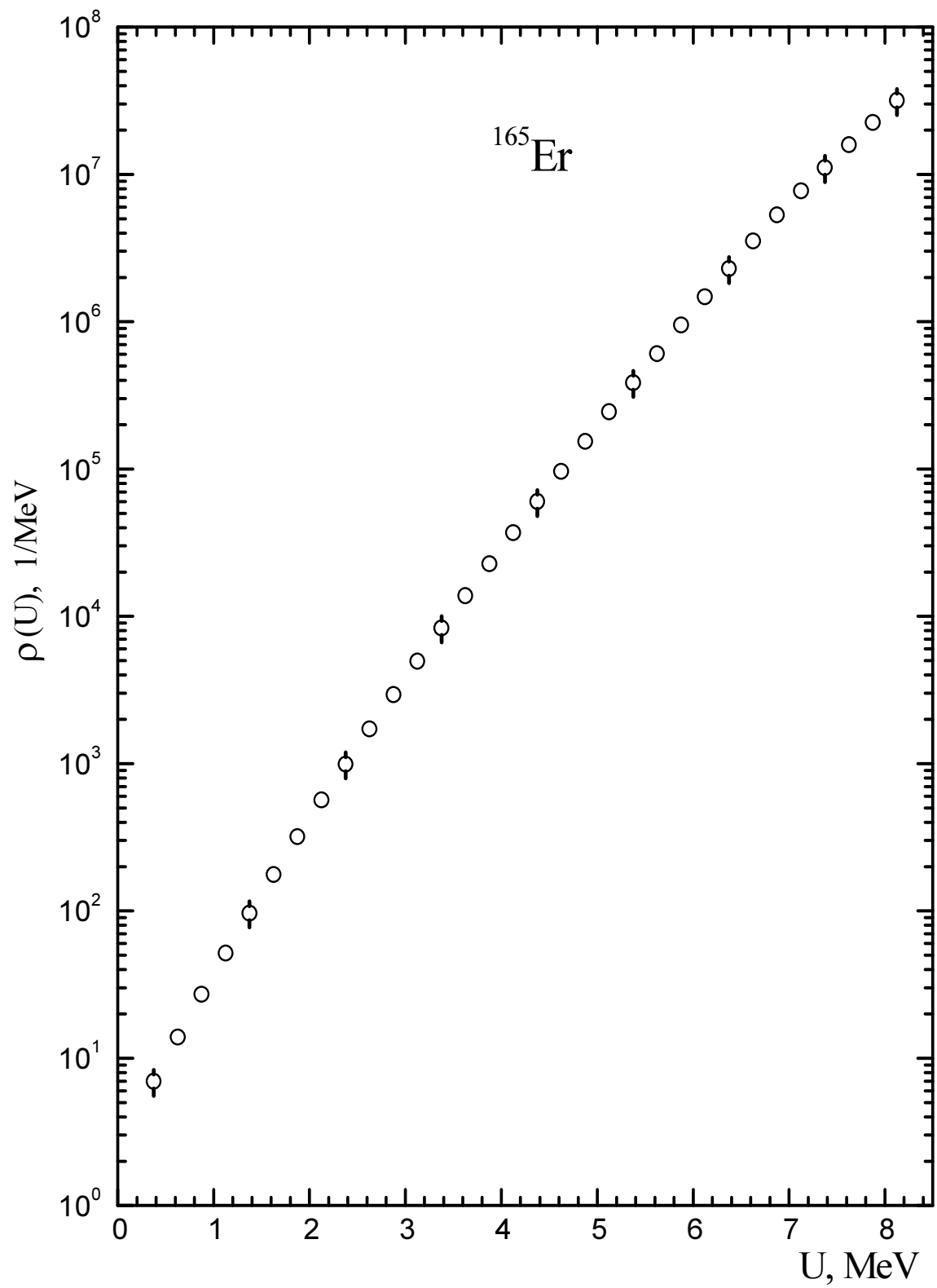


**FIG. 7.** Nuclear level density of  $^{165}\text{Er}$

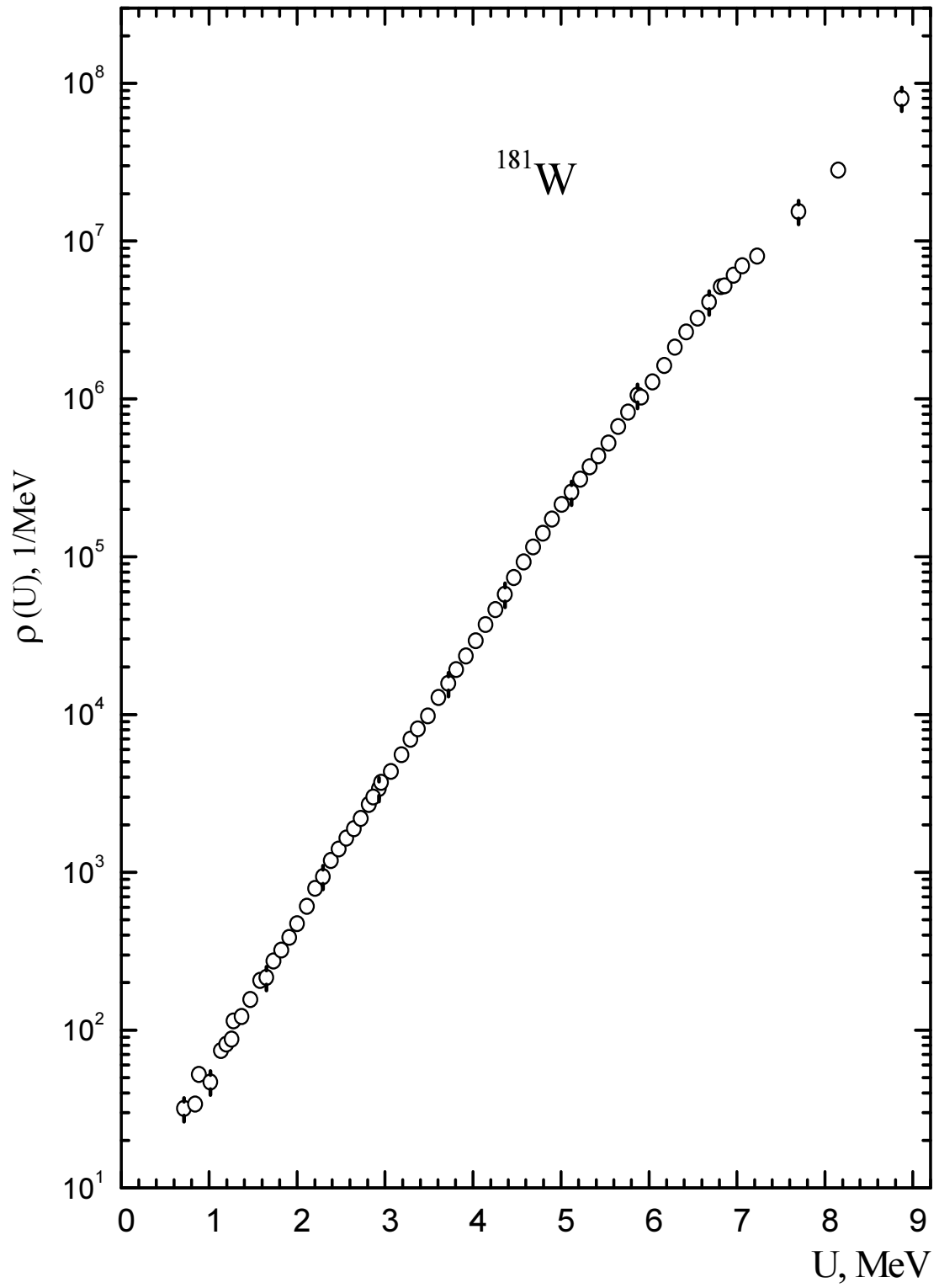


**FIG. 8.** Nuclear level density of  $^{181}\text{W}$

**TABLE 1.** NUCLEAR LEVEL DENSITY OF Sb-116 [1]

U, MeV	$\rho(U)$	$\Delta\rho(U)$	U, MeV	$\rho(U)$	$\Delta\rho(U)$	U, MeV	$\rho(U)$	$\Delta\rho(U)$
0.80	17.06	2.56	2.35	1.45E3	217	3.85	3.00E4	4.49E3
0.85	21.09	3.16	2.40	1.62E3	242	3.90	3.28E4	4.93E3
0.90	25.09	3.76	2.45	1.80E3	271	3.95	3.60E4	5.40E3
0.95	29.07	4.36	2.50	2.01E3	302	4.00	3.94E4	5.92E3
1.00	34.84	5.23	2.55	2.24E3	337	4.05	4.32E4	6.48E3
1.05	43.23	6.49	2.60	2.50E3	375	4.10	4.72E4	7.09E3
1.10	56.39	8.46	2.65	2.78E3	417	4.15	5.17E4	7.75E3
1.15	71.18	10.7	2.70	3.10E3	464	4.20	5.65E4	8.48E3
1.20	70.38	10.6	2.75	3.44E3	516	4.25	6.18E4	9.26E3
1.25	98.42	14.8	2.80	3.82E3	573	4.30	6.75E4	1.01E4
1.30	184.3	27.7	2.85	4.24E3	636	4.35	7.37E4	1.10E4
1.35	264.3	39.7	2.90	4.70E3	705	4.40	8.04E4	1.21E4
1.40	314.3	47.2	2.95	5.21E3	782	4.45	8.78E4	1.32E4
1.45	332.7	49.9	3.00	5.78E3	866	4.50	9.57E4	1.44E4
1.50	372.7	55.9	3.05	6.39E3	959	4.55	1.04E5	1.57E4
1.55	391.5	58.7	3.10	7.07E3	1.06E3	4.60	1.14E5	1.71E4
1.60	401.5	60.2	3.15	7.82E3	1.17E3	4.65	1.24E5	1.86E4
1.65	423.4	63.5	3.20	8.64E3	1.30E3	4.70	1.35E5	2.02E4
1.70	433.4	65.0	3.25	9.54E3	1.43E3	4.75	1.47E5	2.20E4
1.75	451.6	67.7	3.30	1.05E4	1.58E3	4.80	1.60E5	2.40E4
1.80	452.8	67.9	3.35	1.60E4	1.74E3	4.85	1.74E5	2.69E4
1.85	459.8	69.0	3.40	1.28E4	1.92E3	4.90	1.89E5	2.84E4
1.90	512.9	76.9	3.45	1.41E4	2.11E3	4.95	2.05E5	3.08E4
1.95	582.8	87.4	3.50	1.55E4	2.33E3	5.00	2.23E5	3.35E4
2.00	650.3	97.5	3.55	1.71E4	2.56E3	5.05	2.43E5	3.64E4
2.05	726.2	109	3.60	1.88E4	2.82E3	5.10	2.63E5	3.95E4
2.10	815.8	122	3.65	2.06E4	3.10E3	5.15	2.86E5	4.29E4
2.15	916.9	138	3.70	2.27E4	3.40E3	5.20	3.10E5	4.65E4
2.20	1.03E3	154	3.75	2.49E4	3.73E3	5.25	3.37E5	5.05E4
2.25	1.15E3	173	3.80	2.73E4	4.10E3	5.30	3.65E5	5.48E4
2.30	1.29E3	194						

**TABLE 2.** NUCLEAR LEVEL DENSITY OF Sb-118 [1]

U, MeV	$\rho(U)$	$\Delta\rho(U)$	U, MeV	$\rho(U)$	$\Delta\rho(U)$	U, MeV	$\rho(U)$	$\Delta\rho(U)$
0.50	31.87	4.78	2.55	3.70E3	5.55E2	4.60	2.25E5	3.38E4
0.55	34.83	5.22	2.60	4.14E3	6.22E2	4.65	2.47E5	3.70E4
0.60	38.07	5.71	2.65	4.64E3	6.96E2	4.70	2.70E5	4.04E4
0.65	42.07	6.31	2.70	5.16E3	7.78E2	4.75	2.95E5	4.42E4
0.70	45.39	6.81	2.75	5.79E3	8.69E2	4.80	3.22E5	4.83E4
0.75	48.39	7.26	2.80	6.47E3	9.70E2	4.85	3.51E5	5.27E4
0.80	51.09	7.66	2.85	7.21E3	1.08E3	4.90	3.83E5	5.75E4
0.85	55.09	8.26	2.90	8.04E3	1.21E3	4.95	4.18E5	6.28E4
0.90	59.03	8.86	2.95	8.95E3	1.34E3	5.00	4.56E5	6.85E4
0.95	65.03	9.76	3.00	9.97E3	1.50E3	5.05	4.98E5	7.46E4
1.00	70.11	10.5	3.05	1.11E4	1.66E3	5.10	5.42E5	8.14E4
1.05	90.11	13.5	3.10	1.23E4	1.85E3	5.15	5.91E5	8.86E4
1.10	129.3	19.4	3.15	1.37E4	2.05E3	5.20	6.44E5	9.66E4
1.15	200.3	30.1	3.20	152E4	2.28E3	5.25	7.01E5	1.05E5
1.20	280.7	42.1	3.25	1.68E4	2.53E3	5.30	7.63E5	1.14E5
1.25	340.7	51.1	3.30	1.87E4	2.80E3	5.35	8.30E5	1.25E5
1.30	381.0	57.2	3.35	2.07E4	3.10E3	5.40	9.30E5	1.35E5
1.35	406.7	61.0	3.40	2.29E4	3.44E3	5.45	9.82E5	1.47E5
1.40	420.5	63.1	3.45	2.54E4	3.80E3	5.50	1.07E6	1.60E5
1.45	423.8	63.6	3.50	2.80E4	4.21E3	5.55	1.16E6	1.74E5
1.50	424.2	63.6	3.55	3.10E4	4.65E3	5.60	1.26E6	1.89E5
1.55	433.1	65.0	3.60	3.42E4	5.13E3	5.65	1.37E6	2.05E5
1.60	441.5	66.2	3.65	3.78E4	5.67E3	5.70	1.49E6	2.23E5
1.65	440.5	66.1	3.70	4.17E4	6.25E3	5.75	1.61E6	2.42E5
1.70	442.0	66.3	3.75	4.60E4	6.90E3	5.80	1.75E6	2.62E5
1.75	453.7	68.1	3.80	5.07E4	7.60E3	5.85	1.90E6	2.85E5
1.80	480.3	72.1	3.85	5.58E4	8.38E3	5.90	2.06E6	3.09E5
1.85	513.7	77.1	3.90	6.15E4	9.22E3	5.95	2.23E6	3.34E5
1.90	600.4	90.1	3.95	6.77E4	1.02E4	6.00	2.42E6	3.63E5
1.95	823.9	124	4.00	7.44E4	1.12E4	6.05	2.62E6	3.93E5
2.00	1.07E3	160	4.05	8.18E4	1.28E4	6.10	2.84E6	4.25E5
2.05	1.21E3	181	4.10	8.99E4	1.35E4	6.15	3.07E6	4.61E5
2.10	1.34E3	201	4.15	9.88E4	1.48E4	6.20	3.32E6	5.00E5

**TABLE 3.** NUCLEAR LEVEL DENSITY OF Sb-122 [1]

U, MeV	$\rho(U)$	$\Delta\rho(U)$	U, MeV	$\rho(U)$	$\Delta\rho(U)$
0.9	28.95	4.34	4.1	1.56E4	2.33E3
1.0	32.21	4.83	4.2	1.84E4	2.76E3
1.1	38.46	5.77	4.3	2.17E4	3.25E3
1.2	59.54	8.93	4.4	2.55E4	3.83E3
1.3	72.36	10.9	4.5	3.00E4	4.50E3
1.4	90.23	13.5	4.6	3.52E4	5.29E3
1.5	105.2	15.8	4.7	4.13E4	6.20E3
1.6	132.7	19.9	4.8	4.84E4	7.26E3
1.7	158.4	23.8	4.9	5.66E4	8.49E3
1.8	199.2	29.9	5.0	6.61E4	9.91E3
1.9	262.9	39.4	5.1	7.71E4	1.16E4
2.0	326.4	49.0	5.2	8.98E4	1.35E4
2.1	400.5	60.1	5.3	1.04E5	1.57E4
2.2	495.6	74.3	5.4	1.21E5	1.82E4
2.3	577.5	86.6	5.5	1.41E5	2.11E4
2.4	697.7	105	5.6	1.63E5	2.45E4
2.5	845.7	128	5.7	1.89E5	2.84E4
2.6	1.03E3	155	5.8	2.19E5	3.28E4
2.7	1.24E3	186	5.9	2.53E5	3.80E4
2.8	1.51E3	227	6.0	2.92E5	4.38E4
2.9	1.83E3	275	6.1	3.37E5	5.06E4
3.0	2.21E3	331	6.2	3.88E5	5.83E4
3.1	2.67E3	400	6.3	4.47E5	6.71E4
3.2	3.21E3	481	6.4	5.14E5	7.72E4
3.3	3.85E3	578	6.5	5.91E5	8.87E4
3.4	4.62E3	694	6.6	6.79E5	1.02E5
3.5	5.52E3	828	6.7	7.78E5	1.17E5
3.6	6.59E3	989	6.8	8.20E5	1.34E5
3.7	7.86E3	1.18E3	6.9	1.02E6	1.53E5
3.8	9.34E3	1.40E3	7.0	1.17E6	1.75E5
3.9	1.11E4	1.66E3	7.1	1.34E6	2.00E5
4.0	1.31E4	1.97E3	7.2	1.53E6	2.29E5

**TABLE 4.** NUCLEAR LEVEL DENSITY OF Sb-124 [1]

U, MeV	$\rho(U)$	$\Delta\rho(U)$	U, MeV	$\rho(U)$	$\Delta\rho(U)$	U, MeV	$\rho(U)$	$\Delta\rho(U)$	U, MeV	$\rho(U)$	$\Delta\rho(U)$
0.50	30.00	4.50	2.65	958.4	144	4.80	3.00E4	4.50E3	6.95	5.97E5	8.96E4
0.55	30.00	4.50	2.70	1.05E3	158	4.85	3.23E4	4.85E3	7.00	6.37E5	9.56E4
0.60	30.00	4.50	2.75	1.14E3	172	4.90	3.48E4	5.22E3	7.05	6.80E5	1.02E5
0.65	29.87	4.48	2.80	1.25E3	187	4.95	3.75E4	5.63E3	7.10	7.25E5	1.09E5
0.70	30.00	4.50	2.85	1.35E3	202	5.00	4.04E4	6.06E3	7.15	7.73E5	1.16E5
0.75	30.75	4.61	2.90	1.47E3	221	5.05	4.35E4	6.53E3	7.20	8.23E5	1.24E5
0.80	32.00	4.80	2.95	1.65E3	247	5.10	4.69E4	7.03E3	7.25	8.78E5	1.32E5
0.85	34.05	5.10	3.00	1.84E3	276	5.15	5.04E4	7.56E3	7.30	9.35E5	1.40E5
0.90	36.03	5.41	3.05	1.99E3	299	5.20	5.43E4	8.14E3	7.35	9.96E5	1.49E5
0.95	36.71	5.51	3.10	2.15E3	322	5.25	5.83E4	8.75E3	7.40	1.07E6	1.59E5
1.00	38.01	5.70	3.15	2.32E3	348	5.30	6.27E4	9.41E3	7.45	1.13E6	1.69E5
1.05	41.95	6.29	3.20	2.51E3	376	5.35	6.74E4	1.01E4	7.50	1.20E6	1.80E5
1.10	47.01	7.05	3.25	2.71E3	407	5.40	7.25E4	1.09E4	7.55	1.28E6	1.92E5
1.15	52.32	7.85	3.30	2.93E3	439	5.45	7.78E4	1.17E4	7.60	1.36E6	2.44E5
1.20	58.00	8.70	3.35	3.17E3	476	5.50	8.36E4	1.25E4	7.65	1.45E6	2.18E5
1.25	63.71	9.56	3.40	3.42E3	513	5.55	8.98E4	1.35E4	7.70	1.54E6	2.31E5
1.30	70.03	10.51	3.45	3.70E3	555	5.60	9.64E4	1.45E4	7.75	1.64E6	2.46E5
1.35	77.71	11.66	3.50	4.00E3	600	5.65	1.03E5	1.55E4	7.80	1.75E6	2.62E5
1.40	86.00	12.90	3.55	4.32E3	648	5.70	1.11E5	1.66E4	7.85	1.86E6	2.78E5
1.45	94.12	14.12	3.60	4.67E3	701	5.75	1.19E5	1.79E4	7.90	1.97E6	2.96E5
1.50	103.0	15.45	3.65	5.05E3	758	5.80	1.27E5	1.91E4	7.95	2.10E6	3.15E5
1.55	112.6	16.88	3.70	5.46E3	819	5.85	1.37E5	2.05E4	8.00	2.23E6	3.35E5
1.60	125.1	18.76	3.75	5.90E3	885	5.90	1.47E5	2.20E4	8.05	2.37E6	3.56E5
1.65	145.7	21.85	3.80	6.38E3	957	5.95	1.57E5	2.36E4	8.10	2.52E6	3.78E5
1.70	165.9	24.88	3.85	6.89E3	1.03E3	6.00	1.68E5	2.53E4	8.15	2.68E6	4.01E5
1.75	175.5	26.33	3.90	7.45E3	1.12E3	6.05	1.80E5	2.70E4	8.20	2.84E6	4.26E5
1.80	185.1	27.76	3.95	8.06E3	1.21E3	6.10	1.93E5	2.90E4	8.25	3.02E6	4.53E5
1.85	203.1	30.46	4.00	8.71E3	1.31E3	6.15	2.07E5	3.10E4	8.30	3.21E6	4.81E5
1.90	225.6	33.83	4.05	9.41E3	1.41E3	6.20	2.21E5	3.32E4	8.35	3.40E6	5.10E5
1.95	251.6	37.74	4.10	1.02E4	1.53E3	6.25	2.37E5	3.55E4	8.40	3.61E6	4.19E5
2.00	280.4	42.06	4.15	1.10E4	1.65E3	6.30	2.53E5	3.80E4	8.45	3.83E6	7.5130
2.05	309.6	46.43	4.20	1.19E4	1.78E3	6.35	2.71E5	4.06E4	8.50	4.07E6	6.10E5
2.10	342.6	51.40	4.25	1.29E4	1.93E3	6.40	2.90E5	4.35E4	8.55	4.32E6	6.48E5
2.15	385.1	57.77	4.30	1.39E4	2.08E3	6.45	3.10E5	4.65E4	8.60	4.58E6	6.87E5
2.20	428.8	64.33	4.35	1.50E4	2.25E3	6.50	3.31E5	4.97E4	8.65	4.86E6	7.29E5
2.25	462.1	69.31	4.40	1.62E4	2.44E3	6.55	3.54E5	5.31E4	8.70	5.15E6	7.73E5
2.30	500.9	75.14	4.45	1.75E4	2.63E3	6.60	3.78E5	5.67E4	8.75	5.46E6	8.20E5
2.35	562.7	84.41	4.50	1.90E4	2.84E3	6.65	4.04E5	6.06E4	8.80	5.79E6	8.69E5
2.40	631.9	94.80	4.55	2.05E4	3.07E3	6.70	4.31E5	6.47E4	8.85	6.14E6	9.21E5
2.45	698.9	105	4.60	2.21E4	3.32E3	6.75	4.60E5	6.91E4	8.90	6.51E6	9.77E5
2.50	763.5	115	4.65	2.39E4	3.58E3	6.80	4.92E5	7.37E4	8.95	6.90E6	1.04E6
2.55	816.8	123	4.70	2.58E4	3.87E3	6.85	5.25E5	7.87E4	9.00	7.31E6	1.10E6
2.60	875.6	131	4.75	2.78E4	4.17E3	6.90	5.60E5	8.40E4	9.05	7.75E6	1.16E6

**TABLE 5.** NUCLEAR LEVEL DENSITY OF Er-165 [2]

U, MeV	$\rho(U)$	$\Delta\rho(U)$
0.375	6.95	1.39
0.625	13.92	2.78
0.875	27.14	5.43
1.125	51.72	10.3
1.375	96.57	19.3
1.625	177.0	35.4
1.875	319.2	63.8
2.125	566.9	113
2.375	993.0	199
2.625	1.72E3	343
2.875	2.94E3	587
3.125	4.97E3	993
3.375	8.32E3	1.66E3
3.625	1.38E4	2.76E3
3.875	2.27E4	4.54E3
4.125	3.70E4	7.40E3
4.375	6.00E4	1.20E4
4.625	9.65E4	1.93E4
4.875	1.54E5	3.08E4
5.125	2.45E5	4.90E4
5.375	3.86E5	7.72E4
5.625	6.07E5	1.21E5
5.875	9.49E5	1.90E5
6.125	1.48E6	2.96E5
6.375	2.29E6	4.58E5
6.625	3.53E6	7.06E5
6.875	5.31E6	1.06E6
7.125	7.72E6	1.54E6
7.375	1.11E7	2.22E6
7.625	1.59E7	3.18E6
7.875	2.25E7	4.50E6
8.125	3.17E7	6.34E6

**TABLE 6.** NUCLEAR LEVEL DENSITY OF W-181 [3].

U, MeV	$\rho(U)$	$\Delta\rho(U)$	U, MeV	$\rho(U)$	$\Delta\rho(U)$
0.713	31.78	5.40	3.810	1.93E4	3.28E3
0.840	33.94	5.77	3.921	2.35E4	3.99E3
0.884	52.38	8.90	4.032	2.93E4	4.97E3
1.015	46.86	7.97	4.142	3.71E4	6.30E3
1.135	73.93	12.58	4.253	4.62E4	7.85E3
1.197	81.31	13.82	4.363	5.78E4	9.82E3
1.256	87.49	14.87	4.464	7.35E4	1.25E4
1.278	114.4	19.44	4.575	9.26E4	1.57E4
1.368	121.6	20.67	4.685	1.15E5	1.95E4
1.468	156.0	26.52	4.796	1.40E5	2.39E4
1.579	206.0	35.02	4.896	1.73E5	2.94E4
1.650	215.0	36.55	5.007	2.14E5	3.63E4
1.730	274.0	46.58	5.118	2.56E5	4.35E4
1.821	321.2	54.60	5.218	3.09E5	5.26E4
1.911	385.6	65.55	5.325	3.70E5	6.2900
2.001	472.2	80.27	5.425	4.34E5	7.37E4
2.112	607.4	103.3	5.540	5.26E5	8.93E4
2.203	790.0	134.3	5.650	6.68E5	1.13E5
2.293	938.4	159.5	5.761	8.22E5	1.40E5
2.383	1.19E3	201.5	5.872	1.05E6	1.79E5
2.474	1.40E3	238.7	5.911	1.02E6	1.74E5
2.560	1.65E3	279.7	6.042	1.28E6	2.18E5
2.645	1.88E3	319.9	6.172	1.63E6	2.77E5
2.725	2.19E3	372.0	6.293	2.13E6	3.61E5
2.815	2.69E3	456.8	6.424	2.65E6	4.50E5
2.930	3.39E3	576.0	6.555	3.25E6	5.52E5
2.865	3.00E3	509.5	6.685	4.11E6	6.99E5
2.956	3.71E3	631.0	6.816	5.13E6	8.72E5
3.066	4.35E3	738.8	6.860	5.21E6	8.85E5
3.187	5.55E3	942.8	6.961	6.06E6	1.03E6
3.288	6.97E3	1.19E3	7.062	6.95E6	1.18E6
3.372	8.09E3	1.38E3	7.231	8.00E6	1.36E6
3.488	9.78E3	1.66E3	7.701	1.54E7	2.62E6
3.609	1.28E4	2.17E3	8.151	2.81E7	4.78E6
3.720	1.57E4	2.67E3	8.871	8.01E7	1.36E7





---

Nuclear Data Section  
International Atomic Energy Agency  
P.O. Box 100  
A-1400 Vienna  
Austria

e-mail: [services@iaeand.iaea.org](mailto:services@iaeand.iaea.org)  
fax: (43-1) 26007  
telephone: (43-1) 2600-21710  
Web: <http://www-nds.iaea.org>

---